

Journal Pre-proof

Lactoferrin purification and whey protein isolate recovery from cheese whey using chitosan mini-spheres

Daniela B. Hirsch, Lucas M. Martínez Álvarez, Nicolás Urtasun, María F. Baieli, Juan M. Lázaro- Martínez, Romina J. Glisoni, María V. Miranda, Osvaldo Cascone, Federico J. Wolman

PII: S0958-6946(20)30134-5

DOI: <https://doi.org/10.1016/j.idairyj.2020.104764>

Reference: INDA 104764

To appear in: *International Dairy Journal*

Received Date: 21 February 2020

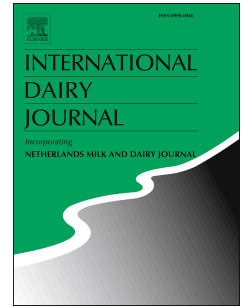
Revised Date: 14 May 2020

Accepted Date: 17 May 2020

Please cite this article as: Hirsch, D.B., Martínez Álvarez, L.M., Urtasun, N., Baieli, M.F., Lázaro-Martínez, J.M., Glisoni, R.J., Miranda, M.V., Cascone, O., Wolman, F.J., Lactoferrin purification and whey protein isolate recovery from cheese whey using chitosan mini-spheres, *International Dairy Journal*, <https://doi.org/10.1016/j.idairyj.2020.104764>.

This is a PDF file of an article that has undergone enhancements after acceptance, such as the addition of a cover page and metadata, and formatting for readability, but it is not yet the definitive version of record. This version will undergo additional copyediting, typesetting and review before it is published in its final form, but we are providing this version to give early visibility of the article. Please note that, during the production process, errors may be discovered which could affect the content, and all legal disclaimers that apply to the journal pertain.

© 2020 Elsevier Ltd. All rights reserved.



1 **Lactoferrin purification and whey protein isolate recovery from cheese whey using chitosan mini-**
2 **spheres**

3
4
5
6 Daniela B. Hirsch^{a,b}, Lucas M. Martínez Álvarez^{a,b,c}, Nicolás Urtasun^{b,d,e}, María F. Baieli^{b,e}, Juan M. Lázaro-
7 Martínez^{f,g}, Romina J. Glisoni^{b,h}, María V. Miranda^{a,b}, Osvaldo Cascone^{a,b}, Federico J. Wolman^{a,b*}

8
9
10
11 ^a *Universidad de Buenos Aires, Facultad de Farmacia y Bioquímica, Cátedra de Biotecnología. Junín 956,*
12 *1113 Buenos Aires, Argentina*

13 ^b *CONICET- Universidad de Buenos Aires, Instituto de Nanobiotecnología (NANOBIOTEC), Junín 956, 1113*
14 *Buenos Aires, Argentina*

15 ^c *Instituto Antártico Argentino, Balcarce 290 3er piso, 1064 Buenos Aires, Argentina*

16 ^d *Universidad de Buenos Aires, Facultad de Ciencias Exactas y Naturales, Departamento de Fisiología,*
17 *Biología Molecular y Celular, Intendente Güiraldes 2160 - Ciudad Universitaria (C1428EGA), Buenos Aires,*
18 *Argentina*

19 ^e *Universidad de Buenos Aires, Facultad de Farmacia y Bioquímica, Junín 956, 1113 Buenos Aires,*
20 *Argentina*

21 ^f *Universidad de Buenos Aires, Facultad de Farmacia y Bioquímica, Departamento de Química Orgánica,*
22 *Junín 956 (C1113AAD), CABA, Argentina.*

23 ^g *CONICET- Universidad de Buenos Aires, Instituto de Química y Fisicoquímica Biológicas (IQUIFIB), Junín*
24 *956 (C1113AAD), CABA, Argentina.*

25 ^h *Universidad de Buenos Aires, Facultad de Farmacia y Bioquímica, Cátedra de Tecnología Farmacéutica*

26 *II. Junín 956, 1113 Buenos Aires, Argentina.*

27

28

29 * Corresponding author. Tel.: +54 11 5287 4679

30 *E-mail address: fwolman@ffyb.uba.ar (F. J. Wolman)*

Journal Pre-proof

31

32 ABSTRACT

33

34 Direct protein purification from raw materials by chromatographic media represents an enormous
35 challenge, especially when particulate solids and high charge solute are present. In this sense, protein
36 purification from cheese whey is an excellent opportunity to test new chromatographic matrices that
37 can be applied to direct protein isolation. The present work shows the utility of novel multimodal
38 chitosan-based chromatographic matrices for obtaining lactoferrin (LF) and a whey protein isolate (WPI)
39 directly from cheese whey without any pretreatment. A central composite experimental design was
40 used to optimise an operative sequence. This sequence involved LF capture using sulfanilic acid-
41 modified chitosan mini-spheres followed by the capture of the massive remnant proteins using glycidyl
42 trimethylammonium-modified chitosan mini-spheres. Interestingly, a yield of 68% and 70% purity
43 degree was obtained for LF, and 2.71 mg of WPI mL⁻¹ whey was obtained in the WPI recovery process,
44 revealing a potential industrial use of the developed matrices and processes.

45

46

47

48 1. Introduction

49

50 Sweet whey is usually applied to food and feed products or commercialised as whey powders;
51 however, a growing interest in its valorisation is mainly due to the high nutritional, biological, and
52 technological value of its proteins and the large volumes produced (Doultani, Turhan, & Etzel, 2003;
53 Mollea, Marmo, & Bosco, 2013; Urtasun et al., 2018).

54 One of the minor proteins present in cheese whey is lactoferrin (LF), which has a concentration
55 of 0.02–0.2 g L⁻¹ and an isoelectric point (pI) higher than 8 (Dizaji, 2016; Etzel, 2004). This protein is
56 commercially interesting because of its role in the innate defence system and its antimicrobial,
57 antioxidant, antiviral, immunomodulating, anti-inflammatory, and anticarcinogenic activities (Garcia-
58 Montoya, Cendon, Arevalo-Gallegos, & Rascon-Cruz, 2012; González-Chávez, Arévalo-Gallegos, &
59 Rascón-Cruz, 2009; Legrand, 2016; Manzoni, 2016; Wakabayashi, Oda, Yamauchi, & Abe, 2014). Due to
60 its high pI compared with other proteins present in cheese whey (Urtasun et al., 2018), it can be
61 selectively adsorbed on cation-exchange materials, which is why ion exchange chromatography is the
62 most common choice for LF purification (Doultani et al., 2003; Pochet et al., 2018; Wakabayashi,
63 Yamauchi, & Takase, 2006). The processing of the remaining whey not only brings economic benefits to
64 the producers but also has a beneficial impact on the environment since the dumping of huge volumes
65 of whey causes environmental pollution (Bacenetti, Bava, Schievano, & Zucali, 2018; Nicolás, Ferreira, &
66 Lassalle, 2019; Price, 2019).

67 Nowadays, two protein products from cheese whey are marketed: whey protein concentrates
68 (WPC) and whey protein isolates (WPI). Protein content in WPC usually varies from 35 to 85%, whereas
69 WPI presents the advantage of having more than 90% protein and almost no carbohydrate content
70 (Kilara & Vaghela, 2018; Nicolás, Ferreira, & Lassalle, 2018). Because of this characteristic, the greatest
71 WPI market is currently intended for sports nutrition, since proteins play an important role in the

72 recovery after arduous exercise and consumers appreciate the absence of carbohydrates in these
73 products (Price, 2019).

74 When processing complex starting materials, such as cheese whey, a pre-treatment is usually
75 necessary before membrane filtration or column chromatography to avoid the fouling of the
76 membranes or the column clogging (Ganju & Gogate, 2017). Some of the strategies used involve
77 chemical, thermal, and ultrasound pre-treatments (Ganju & Gogate, 2017). The use of pre-treatments
78 makes the processing more expensive, which is why using a separation method that avoids this step
79 represents a great advantage. In this regard, our group has already developed several chitosan-based
80 matrices that can be used in batch systems without any pre-treatment due to their size and density
81 (Baieli et al., 2017b; Baieli, Urtasun, Miranda, Cascone, & Wolman, 2014b; Urtasun et al., 2017). Not
82 only do these matrices make the process cheaper but their recovery is facilitated after each step as well.

83 Chitosan is a linear copolymer of 2-acetamide-2-dioxy- β -D-glucose and 2-amino-2-dioxy- β -D-
84 glucose residues randomly distributed. It is the total or partial N-deacetylated derivative form of chitin,
85 which is the second most abundant polysaccharide in nature after cellulose (Kumar, 2000; Kumari,
86 Kumar Annamareddy, Abanti, & Kumar Rath, 2017; Roh & Kwon, 2002). Chitosan presents the
87 advantage of being biodegradable, biocompatible, non-toxic, and highly available (Baieli et al., 2017a;
88 Roh & Kwon, 2002; Shariatinia & Jalali, 2018). In addition, it has many interesting physicochemical
89 properties, like pH sensibility, since it is soluble in dilute acidic media and insoluble in neutral or basic
90 media (Baieli et al., 2017a; Kumar, 2000). This characteristic makes chitosan easy to handle for preparing
91 fibres, hydrogels, micro/nanoparticles, or membranes. Moreover, it presents free amino and hydroxyl
92 groups, which facilitate the immobilisation of various ligands, and is therefore often selected as a
93 support material for chromatographic purposes (Baieli et al., 2017a; Shariatinia & Jalali, 2018; Yang et
94 al., 2016). Regarding this chromatographic purpose, it is well known that chitosan beads or mini spheres
95 formed by the acid/base phase separation possess an open pore internal structure, consisting in macro

96 and meso pores which facilitates protein binding (Subramanian & Hommerding, 2005). Because of its
97 diffusive aspects, regarding protein binding dynamics, this type of chromatographic support has
98 interesting applications in batch operation processes, especially for raw material processing (Baieli,
99 Urtasun, Miranda, Cascone, & Wolman, 2014a).

100 Even though ion exchange chromatography is mostly used in the purification of LF from cheese
101 whey, an appealing alternative is multimodal chromatography (Kallberg, Johansson, & Bulow, 2012;
102 Yang & Geng, 2011; Zhang & Liu, 2016). This type of chromatography consists of ligands that interact
103 with the target proteins in different ways, such as hydrophobic and Van der Waals interactions, in
104 addition to the charge interactions (Johansson et al., 2003; Zhao, Dong, & Sun, 2009). In a previous
105 work, a new multimodal matrix by sulfanilic acid immobilisation on chitosan mini-spheres was
106 developed and characterised (Hirsch et al., 2018a,b). Sulfanilic acid is a precursor in the synthesis of
107 triazine dyes and it presents an aromatic ring in addition to the sulfonic group. Good results in affinity
108 purification processes with these dye-ligands have been studied and reported (Baieli et al., 2014b;
109 Urtasun et al., 2017). An important difference between triazine dyes and their precursor is that the
110 latter does not have regulatory restrictions as a ligand if the purified product or the matrix itself is
111 applied to the food industry. The multimodal matrix developed was successfully tested for lysozyme
112 purification from egg white in a previous study (Hirsch et al., 2018a). Given that LF has a high pI and a
113 complex source, in this study the purification process parameters were optimised through statistical
114 analysis for its purification from cheese whey using the sulfanilic acid-modified chitosan mini-spheres.
115 Another matrix with the opposite charge was also developed to recover WPI. In this sense, quaternary
116 amino groups were introduced in the chitosan mini-spheres by the immobilisation of glycidyl
117 trimethylammonium as the ligand (Prado & Matulewicz, 2014; Senra, Campana-Filho, & Desbrières,
118 2018).

119 The response surface methodology (RSM) has been implemented to optimise the process (Das &
120 Mishra, 2017; Yoshida, 1989). RSM combines mathematical and statistical techniques to improve
121 processes by maximising or minimising (according to the objective set) the response of a variable to
122 several factors (Martínez Álvarez, Lo Balbo, Mac Cormack, & Ruberto, 2015; Ravikumar, Krishnan,
123 Ramalingam, & Balu, 2007). One of the main designs used in chromatography is faced-centred central
124 composite design (CCF) (Kumar Gupta, Agarwal, Asif, Fakhri, & Sadeghi, 2017; Shojaeimehr et al., 2018).
125 RSM is a particularly interesting approach for optimising the chromatographic parameters when using
126 multimodal matrices since many factors are affecting the protein-matrix interactions.

127 Although LF is usually co-purified with lactoperoxidase (LP), this work focuses on LF purification
128 since the market demand for this protein is bigger and it is found at a higher concentration in cheese
129 whey. Despite the number of papers and patents for LF purification, it is still a challenge to purify LF
130 from cheese whey at an industrial scale since not all the proposed technologies are cost-effective. The
131 focus of this work was to purify this protein and take advantage of the remaining whey to further
132 process it through the quantitative isolation of the other whey proteins and study their potential
133 differential elution.

134

135 **2. Materials and methods**

136

137 2.1. *Materials*

138

139 Chitosan (low viscosity, Lot# BCBF7885V, acetylation degree 41%), sulfanilic acid (4-
140 aminobenzenesulfonic acid), and glycidyl trimethylammonium chloride (GTMA) were from Sigma-
141 Aldrich (St. Louis, MO, USA). LF standard (95% purity, 20% iron saturation) was from Friesland Campina
142 Domo® (Amersfoort, The Netherlands). Epichlorohydrin was from Fluka Analytical (Buchs SG,

143 Switzerland). The Bicinchoninic Acid (BCA) protein assay kit for total protein determination was from
144 Thermo Scientific (Rockford, IL, USA). The Bovine Lactoferrin ELISA Quantification kit was from Bethyl
145 Laboratories Inc. (Montgomery, TX, USA). All other reagents were analytical reagent grade.

146

147 2.2. *Sweet whey preparation*

148

149 Milk was kindly donated by Perassolo y Cia. S.A. (Rojas, Buenos Aires, Argentina). Sweet whey
150 was prepared as described in a previous work (Urtasun et al., 2017). Briefly, 0.075 g of chymosin (Sigma-
151 Aldrich) was added to 1 L of milk at 37 °C until coagulation (30 min). Chymosin was inactivated by raising
152 the temperature to 55 °C for 15 min. The resulting whey was centrifuged at 4 °C, 3000 x g, for 30 min to
153 remove the residual fat and the precipitated casein.

154

155 2.3. *Response surface methodology*

156

157 The adsorption and elution steps for the two processes studied were optimised by the CCF
158 design using the Design Expert software (version DX7). Every independent variable was studied in three
159 coded levels (+1, 0, and -1) as shown in Tables 1 and 2. Eq. (1) explains the relation between the coded
160 and the real values:

$$161 \quad x_i = (X_i - X_0)/X \quad (1)$$

162 where X_i is the real value of the independent variable, x_i is the dimensionless coded value for X_i , $i = -1, 0,$
163 $+1$, X_0 is the mid-point of X_i , and X is the step change value.

164 The best-fitting model was selected. Analysis of variance was implemented to validate the
165 model accuracy. Mean squares, lack of fit, sum of squares, F-value, and P -value were the parameters
166 analysed to check the efficacy of the model. P -values confirmed the model from the statistical point of

167 view. According to the variance analysis, P -values lower than 0.05 represented that either the model or
168 the variables were significant from the statistical point of view (95% significance level).

169 For the optimisation of multiple responses, the desirability function ($D(x)$) was maximised
170 according to Eq. (2):

$$171 \quad D(x) = (Y_1 * Y_2 * Y_3 \dots Y_n)^{1/n} \quad (2)$$

172 where Y_i ($i = 1, 2 \dots n$) are the selected responses and n is the total number of responses evaluated. The
173 value of D is between zero (least desirable) and one (most desirable) at the goal set for each response.

174

175 2.4. Matrix synthesis and characterisation

176

177 2.4.1. Matrix synthesis

178 Chitosan mini-spheres (1.32 ± 0.14 mm diameter) were obtained according to the procedure
179 described in previous studies (Baieli et al., 2014b; Hirsch et al., 2018a). Briefly, a chitosan solution was
180 prepared by dissolving 2% of low viscosity chitosan powder (acetylation degree 41%) in 2% acetic acid
181 (Kasaai, Arul, & Charlet, 2000). This solution was dripped through a 30 G needle on a 2 M NaOH solution
182 under continuous soft stirring (Baieli et al., 2014b). The resulting mini-spheres were crosslinked with a
183 250 mM epichlorohydrin solution at 60 °C for 4 h under continuous gentle stirring. The matrix designed
184 for the purification of LF was then activated by a second treatment with epichlorohydrin, using a 2.55 M
185 solution (60 °C, 16 h, pH 10.0) followed by the immobilisation of sulfanilic acid by the reaction with a
186 0.46 M sulfanilic acid solution, pH 10.0, stirred at 60 °C for 40 h. In addition, for the matrix designed for
187 recovering WPI, the 250 mM epichlorohydrin crosslinked mini-spheres were directly incubated with a
188 250 mM GTMA solution in the presence of 0.25% pyridine, pH 10.0, stirred at 60°C for 24 h.

189

190 2.4.2. Nuclear magnetic resonance

191 Solid-state nuclear magnetic resonance (ss-NMR) experiment data were acquired with a Bruker
192 Avance-III HD spectrometer equipped with a 14.1 T narrow bore magnet operating at Larmor
193 frequencies of 600.09 MHz and 150.91 MHz for ^1H and ^{13}C , respectively. Powdered samples were packed
194 into a 3.2 mm ZrO_2 rotor and rotated at room temperature at the magic angle spinning (MAS) rate of 15
195 kHz. The contact time during crosspolarisation (CP) was 2000 μs . The SPINAL64 sequence (small phase
196 incremental alternation with 64 steps) was used for heteronuclear decoupling during acquisition.
197 Spectral editing with the pulse sequence for cross-polarisation with polarisation inversion (CPPI) was
198 used according to previous reports (Algarra et al., 2019; Wu & Zilm, 1993). ^{13}C natural abundance direct
199 polarisation experiments with proton decoupling (SPINAL64) during acquisition were conducted for the
200 GTMA-chitosan sample. An excitation pulse of 4.0 μs and a recycling time of 100 s were used and 4000
201 scans were accumulated to obtain quantitative and good signal-to-noise ratio.

202

203 2.4.3. Zeta potential

204 The ζ potential study was performed as previously reported (Hirsch et al., 2018a). Briefly, the
205 matrices were first disrupted mechanically (100 mg 10 mL^{-1} distilled water) with a spatula and then kept
206 under magnetic stirring for 48 h to obtain a homogeneous microparticle suspension. The particle size
207 was homogenised by filtrating the suspensions (1.2 mm nitrocellulose membrane, Osmonics). Aliquots
208 (2 mL) were diluted 1:1 with distilled water, and NaCl was added until a 10 mM solution concentration
209 was obtained. An adequate volume of 50 mM HCl or NaOH solution was added to adjust the pH value in
210 a range between 2.0 and 9.0.

211 The hydrodynamic size (D_h), size distribution (polydispersity index, PDI), and ζ potential of the
212 different samples were assayed by dynamic light scattering using a Zeta sizer Nano-ZS (Malvern
213 Instruments, Malvern, UK) at a scattering angle of 173° and a fixed measurement position of 4.65 mm.

214 The temperature was controlled at 25 ± 0.1 °C (all samples). Viscosities ranged between 0.8875 and
215 0.8888 cP (25 °C), and the refractive index (RI) was 1.33.

216

217 2.5. *Lactoferrin purification*

218

219 2.5.1. *Lactoferrin adsorption isotherms*

220 LF solutions (1 mL) of different concentrations (0.063 – 10 mg mL⁻¹) were incubated with 50 mg of
221 hydrated and buffer-equilibrated matrix with gentle agitation (16 h, 20 °C). The LF solutions were
222 prepared at different pH values using 20 mM phosphate buffer for pH 6.0, 7.0, and 8.0, and 20 mM
223 carbonate buffer for pH 9.0 with gentle agitation (16 h, 20 °C). The adsorbed equilibrium protein
224 concentration was calculated from the difference between the initial and final LF concentrations
225 measured at 280 nm using the extinction coefficient factor of 1.51. The results were analysed by the
226 Langmuir model (Langmuir, 1917).

227 Langmuir isotherm can be expressed by the following equation (3):

$$228 \quad q = q_m C / (K_d + C) \quad (3)$$

229 where q is the adsorbed protein mass at equilibrium, q_m is the maximum adsorption capacity, C is the
230 protein concentration in the solution at equilibrium, and K_d is the dissociation constant.

231 All determinations were performed in triplicate, and the results were expressed as the average \pm
232 SD.

233

234 2.5.2. *Adsorption studies from whey*

235 For the adsorption, three independent variables were taken into account: amount of hydrated
236 matrix (mg) (A), adsorption time (h) (B), and whey pH (C).

237 Six central points (0,0,0) were included in the analysis, resulting in 20 experiments to be
238 performed (Supplementary material Table S1). Only one response was analysed: LF adsorption (R1LFA).
239 The response was defined by the following equation (4):

$$240 \quad R1LFA (\%) = [LF \text{ adsorbed (mg)} * 100] / [LF \text{ in the initial whey (mg)}] \quad (4)$$

241 The objective was to optimise this process by maximising R1LFA. The mini-spheres were first
242 equilibrated with a buffer set at the same pH as that of the adsorption step, followed by the adsorption
243 at the condition determined by the design. All experiments were performed at 11 °C to reduce the
244 growth of microorganisms. The results were determined by the Bovine Lactoferrin ELISA Quantification
245 kit and the BCA protein assay kit for total protein determination.

246

247 2.5.3. Elution studies

248 For the elution step, three independent variables were taken into account: elution buffer pH (A),
249 NaCl molar concentration (B), and propylene glycol (PG) percentage (C). The pH and NaCl concentration
250 would mainly affect the ionic interactions between the matrix and the protein; however, the PG and the
251 pH would alter the hydrophobic interactions.

252 As for adsorption, six central points (0,0,0) were included in the analysis, resulting in 20
253 experiments (Table S1). Two responses were analysed: LF elution (R2LFE) and total proteins eluted
254 (R3LFE). These responses were defined by the following equations (5 & 6):

$$255 \quad R2LFE (\%) = [LF \text{ eluted (mg)} * 100] / [LF \text{ adsorbed (mg)}] \quad (5)$$

$$256 \quad R3LFE (\%) = [Total \text{ proteins eluted (mg)} * 100] / [Total \text{ proteins in the initial whey (mg)}] \quad (6)$$

257 The objective was to optimise this process by maximising R2LFE while R3LFE was set at a target
258 of 1.59%, which is the amount of LF in the original whey, to achieve higher purity in the eluent.

259 The mini-spheres were first equilibrated with 20 mM phosphate buffer, pH 7.0, followed by the
260 adsorption at the optimal condition previously determined in the adsorption study. Four washing steps

261 were included after the adsorption using 20 mM phosphate buffer, pH 7.0, and the elution buffer was
262 determined according to the experimental design. The results were measured as previously described.

263

264 2.5.4. Purification of lactoferrin from cheese whey

265 To verify the results obtained from the RSM study, a purification process under the optimal
266 conditions found by RSM for adsorption and elution was performed in batch mode. The mini-spheres
267 (100 mg mL⁻¹ of whey) were first equilibrated using 20 mM phosphate buffer, pH 6.7. The adsorption
268 step was performed at the original pH of the cheese whey (6.6), 11 °C for 4 h with gentle stirring. Four
269 washing steps were carried out with the equilibration buffer, and 20 mM phosphate buffer (pH 7.5)
270 solution with 1.45 M NaCl and 31.33% of PG were used for the elution. LF and total protein
271 concentration were determined as previously described and analysed by SDS-PAGE.

272

273 2.6. Whey protein isolate recovery

274

275 2.6.1. Adsorption studies

276 For the adsorption, two independent variables were taken into account: amount of hydrated
277 matrix (mg) (A) and adsorption time (h) (B).

278 Five central points (0,0) were included in the analysis, resulting in 14 experiments to be
279 performed (Supplementary material Table S2). Only one response was analysed: Total protein
280 adsorption (R4WPIA), which was defined by the following equation (7):

$$281 \quad R4WPIA (\%) = [Total\ proteins\ adsorbed\ (mg) * 100] / [Total\ proteins\ in\ the\ initial\ whey\ (mg)] \quad (7)$$

282 The objective was to optimise this process by maximising R4WPIA. All experiments were
283 performed at 11 °C. The results were determined by the BCA protein assay kit.

284

285 2.6.2. Elution studies

286 For the elution, three independent variables were taken into account: elution buffer pH (A),
287 NaCl molar concentration (B), and PG percentage (C). Six central points (0,0,0) were included in the
288 analysis, resulting in 20 experiments to be performed (Supplementary material Table S1). Only one
289 response was analysed: total proteins eluted (R5WPIE). This response was defined by the following
290 equation (8):

$$291 \quad R5WPIE (\%) = [Total\ proteins\ eluted\ (mg) * 100] / [Total\ proteins\ in\ the\ initial\ whey\ (mg)] \quad (8)$$

292 The objective was to optimise this process by maximising R5WPIE. The mini-spheres were first
293 equilibrated with 20 mM phosphate buffer, pH 7.0, followed by the adsorption at the optimal condition
294 found in the adsorption study at 11 °C. Four washing steps were included after the adsorption using the
295 equilibration buffer, and the elution buffer was selected according to the experimental design. Total
296 protein was measured using the BCA protein assay kit. In addition, the eluents were analysed by HPLC to
297 determine if any tested condition allowed the elution of a specific protein.

298

299 2.6.3. Recovery of whey protein isolate from cheese whey

300 The optimum conditions found in the adsorption and elution RSM studies were verified in a
301 recovery process. The mini-spheres (1000 mg mL⁻¹ of whey) were first equilibrated using 20 mM sodium
302 phosphate buffer, pH 7.0. The adsorption step was performed at 11 °C with gentle stirring for 0.5 h. Four
303 washing steps were conducted using the equilibration buffer. A 20 mM sodium acetate buffer, pH 4.0,
304 with 1.57 M NaCl and 50.0 % of PG was used for the elution. LF and the total protein concentration were
305 determined as previously described and analysed by SDS-PAGE. The lactose concentration was
306 measured in the eluents by an enzymatic methodology.

307

308 2.7. Lactose determination

309

310 The lactose determination was performed according to the enzymatic methodology (Ansari,
311 Satar, Kashif Zaidi, & Ahmad, 2014; Mariotti, Yamanaka, Araujo, & Trevisan, 2008). These samples were
312 incubated at 45 °C for 30 min, an aliquot of 10 µL was taken from each sample, and the glucose
313 concentration was determined using an enzymatic glycaemic kit. The glucose concentration was also
314 determined for the samples evaluated without β-galactosidase; all sample absorbances were read at
315 505nm in UV-Visible spectrophotometer (Shimadzu Inc., Kyoto, Japan). Glucose concentration was
316 calculated by comparison with standard glucose concentrations. The lactose moles on each sample were
317 determined according to the following equation (9):

$$318 \quad \text{Lactose moles of the sample} = \text{Glucose moles from the sample with } \beta \text{ galactosidase} - \text{Glucose} \\ 319 \quad \text{moles of the sample without treatment} \quad (9)$$

320 All determinations were performed in triplicate, and the results were expressed as the average ±
321 SD.

322

323 3. Results and discussion

324

325 3.1. Matrix synthesis and characterisation

326

327 It is worth mentioning that, from the same original material, two similar syntheses resulted in
328 different chitosan-based chromatographic materials (Fig. 1), providing evidence of the expanding uses of
329 this natural polymer in chromatographic applications.

330 To obtain chemical information about the modification of chitosan with GTMA, ¹³C ss-NMR
331 experiments were done and the results are shown in Fig. 2. The ¹³C CP-MAS spectrum for the GTMA-
332 modified chitosan mini-spheres shows the carbon resonance signals for the chitosan structure (C₁₋₈) and

333 those for the crosslinking with epichlorohydrin (C₉₋₁₀) (Hirsch et al., 2018a) and with the reaction with
334 GTMA (C₁₁₋₁₄). Particularly, the ¹³C CPPI experiment allowed us to unequivocally assign the methyl
335 carbons of the trimethylammonium group of the GTMA at a carbon chemical shift of 54.9 ppm
336 (Supplementary material Fig. S1). Considering that this signal is representative of the GTMA moieties in
337 the chitosan mini-spheres, a ¹³C direct polarisation experiment was conducted using a sufficiently long
338 recycle delay for all the ¹³C to relax. In this sense, the quantitative amount of GTMA related to the
339 chitosan structure can be estimated from the deconvolution of the ¹³C-NMR line (Supplementary
340 material Fig. S1). The quantitative information for the GTMA mini-spheres estimated that every three
341 monomeric units of chitosan one was modified. The difference observed between the ¹³C CP-MAS and
342 ¹³C DP spectra stemmed from the intensity of the NMR lines from the ordered or crystalline regions
343 enhanced in the cross-polarisation experiment (Lázaro-Martínez, Rodríguez-Castellón, Vega, Monti, &
344 Chattah, 2015). However, the direct-polarisation experiment with an adequate long recycle delay can
345 bring quantitative information from the NMR lines of the entire system (ordered or disordered regions).
346 In the latter region, the only disadvantage is the time consumed by the spectrometer to obtain a good
347 signal-to-noise ratio (5 days for the GTMA-chitosan sample).

348 The ζ potential curves versus pH (Fig. 3) reveal that the incorporation of the different ligands
349 was successful. The immobilisation of the sulfonic groups onto the chitosan mini-spheres showed a
350 charge inversion at a pH-value between 5 and 6. However, the immobilisation of the GTMA showed an
351 increase in the charge in almost all the pH spectrum.

352

353 3.2. *Lactoferrin purification*

354

355 3.2.1. *Equilibrium adsorption isotherms*

356 Maximum adsorption capacity (q_m) was determined following the Langmuir model from the
 357 equilibrium adsorption isotherms. To characterise the interaction between LF and the matrix, q_m was
 358 determined at different pH values at which the matrix has a net negative charge (6.0–9.0). Fig. 4 shows
 359 that the highest q_m was reached at pH 8.0 ($112.4 \pm 6.347 \text{ mg g}^{-1}$). However, there was no linear relation
 360 between the pH value and the measured q_m , which may be attributed to the interaction between the
 361 matrix and the protein not being entirely mediated by ion exchange, thus revealing other types of
 362 interactions that are not negligible.

363 Compared with other ion exchange matrices, the maximum adsorption capacity obtained was
 364 high. In a previous work, LF isolation from bovine colostrum was studied using a cation exchange resin
 365 SPEC 70 SLS from Pall Corporation (Port Washington, New York, USA). In this case, the maximum
 366 adsorption capacity resulted in 21.73 mg g^{-1} resin at pH 7.0 (Liang, Wang, Wu, & Zhu, 2011).

367

368 3.2.2. Adsorption studies

369 The response, R1LFA, was analysed as shown in Fig. 5 and it followed Eq. 10, in terms of codified
 370 factors (A = amount of hydrated matrix (mg); B = adsorption time (h); C = whey pH).

$$371 \quad R1LFA = +52.68 + 24.79 * A + 16.86 * B + 9.51 * C - 3.14 * A * B - 5.82 * A * C - 7.78 * B * C -$$

$$372 \quad 6.33 * A^2 - 9.12 * B^2 - 0.72 * C^2 \quad (10)$$

373 Supplementary material Table S3 presents the ANOVA results for R1LFA. The optimum
 374 adsorption conditions were obtained using numerical optimisation of RSM, to attain the maximum LF
 375 adsorption (R1LFA). The optimum amount of hydrated matrix was 100 mg, adsorption time 4 h, and pH
 376 6.57. The predicted value for R1LFA was 78.00%. As the pH of the cheese whey is 6.60, this factor was
 377 left unmodified. At pH 6.57, the matrix and most of the proteins were charged negatively, while the
 378 target protein had the opposite charge (Urtasun et al., 2018). This factor is also seen as important in Fig.
 379 4 since it influenced the maximum capacity of the matrix.

380 When analysing the other two variables (adsorption time and amount of matrix), it is important
 381 to take into account that adsorption time is usually limited to increase the process productivity and to
 382 reduce the growth of microorganisms in the remaining whey. For this reason, the maximum adsorption
 383 time studied was 4 h. Noteworthy, when working with batch systems, diffusion is the main time
 384 limitation since the target molecule has to diffuse from the solution to the hydrated film around the
 385 adsorbent, then inside the pore, and afterward interact according to its binding kinetics (Urtasun et al.,
 386 2018). Given that LF is at a low concentration compared with other proteins in the cheese whey, the
 387 limitation of 4 h for the adsorption may influence the amount of matrix needed to accomplish the
 388 adsorptive step, which could explain not only the significance of this variable but also the fact that the
 389 optimum for both variables was near the higher level.

390

391 3.2.3. Elution studies

392 The first response analysed was R2LFE, as shown in Fig. 6A, and it followed Eq. 11, in terms of
 393 coded factors (A = elution buffer pH; B = NaCl molar concentration; C = propylene glycol percentage).

$$394 \quad R2LFE = +68.95 + 12.54 * A + 24.64 * B + 13.85 * C + 13.57 * A * B - 0.26 * A * C + 11.82 * B * C -$$

$$395 \quad 7.94 * A^2 - 25.56 * B^2 - 13.75 * C^2 \quad (11)$$

396 Supplementary material Table S4 presents the ANOVA results for R2LFE. The second response
 397 was R3LFE and it followed Eq. 12 in terms of the same codified factors described for Eq. 11 (Fig. 6B).

$$398 \quad R3LFE = +1.99 + 0.42 * A + 1.27 * B + 0.30 * C + 0.48 * A * B + 0.70 * A * C + 0.46 * B * C + 0.52 *$$

$$399 \quad A * B * C \quad (12)$$

400 Supplementary material Table S5 shows the ANOVA results.

401 The optimum pH was 7.53, NaCl concentration was 1.33 M, and PG was 32.42%. The predicted
 402 values for R2LFE and R3LFE were 84.98% and 2.97%, respectively, with desirability of 0.840 as shown in
 403 Fig. 6C. Fig. 6A,B indicates that, for the same pH value, both responses were maximised using the

404 maximum PG and NaCl concentrations; however, since the curvatures of the plots differ from one
405 another, it was possible to obtain a result with good desirability. Even though the composition of the
406 starting material is very important in the optimisation of these variables and a study is required in each
407 individual case, the information from this study, in particular, allows a proper definition of the limits of
408 each variable to obtain more certain information and reduce the time and number of experiments
409 required for process development.

410 The fact that the terms NaCl and PG were significant for R2LFE suggests that the interaction
411 between the mini-spheres and the target protein is mediated both by ion exchange and hydrophobic
412 interactions. However, in Eq. 11, the coefficient for the NaCl factor is larger than that for the PG factor,
413 which means that ion exchange forces are predominant over the hydrophobic ones. The variable NaCl is
414 the most significant for both responses, as shown by Eqs. 11 and 12, the NaCl (B) terms have the larger
415 number and are positive for both responses. This makes it more difficult to set the optimum for this
416 variable to accomplish the objective, which is to maximise one response while the other one is targeted
417 at 1.59%. For this reason, for the optimisation step, the two responses were given different levels of
418 importance: R2LFE maximisation was highly important (+++++) while R3 minimisation was left at a
419 medium setting of importance (+++) (Fan, Duquette, Dumont, & Simpson, 2018). Given that R2LFE
420 presents B^2 as a significant term (Supplementary material Table S4) with a negative effect on the
421 response, the optimum for this term was not the highest but 0.33 in coded factors.

422 Regarding the role of pH in the elution, although this variable is not significant for R2LFE, the
423 interaction between the pH and the PG was significant for R3LFE. As the term in Eq. 12 is positive, if this
424 were the only response considered and the objective was to minimise it (because the target was low),
425 one of the two factors (A or C) would need to have a negative coded number. Nonetheless, because of
426 the greater importance established for R2LFE, this information is not seen in the optimum reached.

427

428 3.2.4. Purification of lactoferrin from cheese whey

429 The predicted optimums obtained from the RSM for the adsorption and the elution were used in
430 a process to verify the correspondence between the predicted and the actual values. The differences
431 between the predicted value and the actual responses were as follows: 1.49% for Adsorption R1LFA
432 (78.00% and 76.51%, respectively), 4.49% for Elution R2LFE (84.98% and 89.47%, respectively), and
433 0.46% for Elution R3LFE (2.97% and 2.51%, respectively). These results show that there was no
434 significant difference between the actual and the predicted values ($p > 0.05$). The complete purification
435 process showed a purification factor of 27.52 ± 0.21 and a yield of 67.99 ± 1.12 %. Fig. 7 shows the SDS-
436 PAGE of the process. A 70 % purity degree was estimated for LF by gel densitometry, which was similar
437 to the commercial food-grade product (lane 1).

438 In comparison with other ion-exchange matrices developed, the results obtained for the mini-
439 spheres were similar to previous results obtained from different methods, but in this case no pre-
440 treatment was necessary and the recovery of the matrix after each purification step was easily done
441 with a sieve. For instance, other authors used carboxymethyl ion-exchange chromatography for LF
442 purification from acid cheese whey and obtained a yield of 88 mg of LF from 1 L of acid whey (Yoshida &
443 Ye, 1991). However, in their work, hydrophobic chromatography was performed before the ion-
444 exchange chromatography as whey pre-treatment. In the present case, the obtained amount of LF was
445 120 mg from 1 L of cheese whey and no pre-treatment was required. Fractionation of LF was also
446 studied using a microporous membrane containing immobilised sulfonic acid moieties (Chiu & Etzel,
447 1997). A 50 ± 5 % yield was obtained, which is also lower than that obtained with the mini-spheres here
448 presented. In addition, the purification using microporous membranes required a vacuum filtration
449 through a $0.7 \mu\text{m}$ glass filter before the adsorption step.

450

451 3.3. Whey protein isolate recovery

452

453 *3.3.1. Adsorption studies*

454 The response, R4WPIA, was analysed and optimised according to the obtained model. The
455 response followed Eq. 13, in terms of coded factors (A = amount of hydrated matrix (mg); B = adsorption
456 time (h)).

$$457 R4WPIA = +46.53 + 20.83 * A + 2.54 * B \quad (13)$$

458 Supplementary material Table S6 presents the ANOVA results for R4WPIA.

459 The optimum conditions for the adsorption were obtained by RSM numerical optimisation, to
460 attain the maximum total protein adsorption (R4WPIA). The optimum amount of hydrated matrix was
461 1000 mg and the adsorption time was 0.5 h. The predicted value for R4WPIA was 64.82%. This optimum
462 can be analysed from Fig. 8, which clearly shows that, for total proteins to be maximised, the most
463 important factor to be taken into account is the utilisation of the maximum amount of matrix. If the
464 amount of matrix used for the WPI recovery process is compared with the optimum amount for the LF
465 purification, the amount of matrix is only 10 times greater while the total number of whey proteins is by
466 far more than 10 times the total amount of LF (cheese whey has 0.02–0.2 g L⁻¹ of LF and 6 g L⁻¹ of total
467 proteins). Even though a higher amount of matrix is needed to obtain higher adsorption rates, the
468 proper agitation of the system is not possible with a greater amount of matrix. Other authors working in
469 WPI recovery used similar amounts of resin to process an equivalent amount of whey (Gerberding &
470 Byers, 1998).

471

472 *3.3.2. Elution studies*

473 The response analysed followed Eq. 14, in terms of codified factors (A = elution buffer pH; B =
474 NaCl molar concentration; C = propylene glycol percentage) (Fig. 9).

$$R5WPIE = +60.19 - 3.25 * A + 27.76 * B + 1.44 * C - 0.047 * A * B - 1.71 * A * C + 0.99 * B * C - 2.18 * A^2 - 25.46 * B^2 - 1.29 * C^2 \quad (14)$$

Supplementary material Table S7 presents the ANOVA results for R5WPIE. The optimum adsorption conditions were obtained by numerical optimisation of RSM, to attain the maximum total protein elution. The optimum pH was 4.00, the NaCl concentration was 1.57 M, and the PG was 50.0%. The predicted value for R5WPIE was 71.27%.

The fact that the term NaCl was significant for R5WPIE suggests that the interaction between the mini-spheres and the target proteins is mainly by ion exchange. As expected, this model also suggests that using higher pH for the eluent minimises the total proteins eluted. When analysing the PG effect on the elution, we noted that this factor had a low effect on the response. However, if a constraint were to be set to minimise this factor, the response would decrease its predicted value to 63.81%. If this process were scaled-up, an economic evaluation would have to be made to analyse which option would result in a higher profit.

Further studies were made on the eluted fractions to determine if any tested condition resulted in the purification or enrichment of a single whey protein. This analysis was done by HPLC, but none of the conditions tested resulted in a single peak chromatogram (data not shown). All the fractions kept the same peak profiles, where only differences in the total number of proteins were evident.

3.3.3. Recovery of whey protein isolate from cheese whey

The predicted optimums obtained from the RSM for the adsorption and elution were used in a process to verify the correlation between the prediction and the experimental values. The differences between the predicted value and the actual responses were 2.11% for Adsorption R4WPIA (64.82% and 62.71%, respectively) and 5.44% for Elution R5WPIE (71.27% and 65.83%, respectively). These results show that there was no significant difference between the actual and the predicted values ($p > 0.05$).

499 The complete purification process showed a yield of $65.82 \pm 2.20\%$. Fig. 10 shows the SDS-PAGE of the
500 process. The lactose concentration in the eluent was zero.

501 To establish the whole process sequence, the LF content and the total number of whey proteins
502 were evaluated. Interestingly, during the adsorption, 43.81% of the total LF was adsorbed to the matrix.
503 This information was vital in determining the correct sequence of processes for these matrices; thus, the
504 adsorption of LF was defined as the first step of the whole process.

505

506 3.4. *Sequence purification of lactoferrin and whey protein isolate*

507

508 Due to the high loss of LF in the WPI adsorption step and the higher market value of this product
509 in comparison with WPI, the purification of LF was considered the first step in whey processing. The
510 optimum conditions obtained from each purification process were used in the sequence purification,
511 using the pass-through of the LF adsorptive step as a starting material for WPI recovery. Table 3 shows
512 the results of the entire process, where the addition of the LF purification process prior to the WPI
513 purification did not significantly affect the yield of this second process. As can be estimated from this
514 table, a yield of 62.31% was obtained for LF. Regarding WPI, 2.71 mg of whey protein was obtained per
515 ml processed. It is worth mentioning that during LF adsorption, about 0.69 mg of the total protein
516 content was bound to the sulfanilic matrix, and this could explain the slight reduction in the yield
517 obtained for WPI, a reduced content in the initial total protein amount in the LF depleted cheese whey.
518 Lactose concentration was determined for the eluents of the processes, with the absence of this
519 carbohydrate found for both LF and WPI.

520

521 4. **Conclusions**

522

523 The present work provides a useful tool to infer the optimum conditions for the purification
524 process of LF from cheese whey. For this purpose, the matrix developed was applied to use this protein
525 as an ingredient in other formulations and allow the rest of the whey to continue with its usual
526 processing, such as WPI production. The depletion of LF from the cheese whey did not significantly
527 affect the yields of the WPI process, resulting in a higher profit of the total cheese whey processing. This
528 work also focuses on the addition of commercial value of natural polymers, such as chitosan, and its
529 potential use in industrial whey processing. In addition, the fact that the LF purification process has little
530 effect on the composition of the remaining whey, its usual industrial processing and other purification
531 strategies to produce WPI or other products can be considered. Furthermore, the experimental
532 procedure using RSM could be applied to other proteins from other sources using other types of
533 chromatographic supports, being especially interesting for multimodal matrices. The developed mini-
534 spheres allow the cheese whey to be processed without any previous conditioning, to have good
535 mechanic resistance, and to be easily recovered after adsorption/washing and elution steps.

536

537 **Acknowledgements**

538

539 This work was supported by grants from Agencia Nacional de Promoción Científica y Tecnológica
540 de la República Argentina (PICT 2014-2340, PICT 2017-0845) and Universidad de Buenos Aires (UBACYT
541 20020170100023BA). DBH is a CONICET fellow. LMMA is a fellow of Instituto Antártico Argentino. NU,
542 MFB, JMLM, RJG, MVM, OC, and FJW are CONICET career researchers.

543

544 **References**

545

- 546 Algarra, M., Bartolić, D., Radotić, K., Mutavdžić, D., Pino-González, M. S., Rodríguez-Castellón, E., et al.
547 (2019). P-doped carbon nano-powders for fingerprint imaging. *Talanta*, *194*, 150–157.
- 548 Ansari, S. A., Satar, R., Kashif Zaidi, S., & Ahmad, A. (2014). Immobilization of *Aspergillus oryzae* β -
549 galactosidase on cellulose acetate-polymethylmethacrylate membrane and its application in
550 hydrolysis of lactose from milk and whey. *International Scholarly Research Notices*, 2014, Article
551 163987.
- 552 Bacenetti, J., Bava, L., Schievano, A., & Zucali, M. (2018). Whey protein concentrate (WPC) production:
553 Environmental impact assessment. *Journal of Food Engineering*, *224*, 139–147.
- 554 Baieli, M., Urtasun, N., Miranda, M., Cascone, O., & Wolman, F.J. (2014a). Isolation of lactoferrin from
555 whey by dye-affinity chromatography with Yellow HE-4R attached to chitosan mini-spheres.
556 *International Dairy Journal*, *39*, 53–59.
- 557 Baieli, M. F., Urtasun, N., Hirsch, D. B., Bracco, L. F., Miranda, M. V., Cascone, O., et al. (2017a). The use
558 of chitosan mini-spheres for high value protein purification from raw materials. In J. Phillips
559 (Ed.), *Chitin: Properties, applications and research*. New York, NY, USA: Nova Science Publishers
560 Inc.
- 561 Baieli, M. F., Urtasun, N., Martinez, M. J., Hirsch, D. B., Pilosof, A. M. R., Miranda, M. V., et al. (2017b).
562 Affinity chromatography matrices for depletion and purification of casein glycomacropeptide
563 from bovine whey. *Biotechnology Progress*, *33*, 171–180.
- 564 Baieli, M. F., Urtasun, N., Miranda, M. V., Cascone, O., & Wolman, F. J. (2014b). Bovine lactoferrin
565 purification from whey using Yellow HE-4R as the chromatographic affinity ligand. *Journal of*
566 *Separation Science*, *37*, 484–487.
- 567 Chiu, C. K., & Etzel, M. R. (1997). Fractionation of lactoperoxidase and lactoferrin from bovine whey
568 using a cation exchange membrane. *Journal of Food Science*, *62*, 996–1000.

- 569 Das, A., & Mishra, S. (2017). Removal of textile dye reactive green-19 using bacterial consortium:
570 Process optimization using response surface methodology and kinetics study. *Journal of*
571 *Environmental Chemical Engineering*, 5, 612–627.
- 572 Dizaji, N. F. (2016). *Minor whey protein purification using ion-exchange column chromatography*. Ph.D.
573 Thesis. Ontario, Canada: The University of Western Ontario.
- 574 Doultani, S., Turhan, K. N., & Etzel, M. R. (2003). Whey protein isolate and glycomacropeptide recovery
575 from whey using ion exchange chromatography. *Journal of Food Science*, 68, 1389–1395.
- 576 Etzel, M. R. (2004). Manufacture and use of dairy protein fractions. *Journal of Nutrition*, 134, 996S–
577 1002S.
- 578 Fan, H. Y., Duquette, D., Dumont, M. J., & Simpson, B. K. (2018). Salmon skin gelatin-corn zein composite
579 films produced via crosslinking with glutaraldehyde: Optimization using response surface
580 methodology and characterization. *International Journal of Biological Macromolecules*, 120,
581 263–273.
- 582 Ganju, S., & Gogate, P. R. (2017). A review on approaches for efficient recovery of whey proteins from
583 dairy industry effluents. *Journal of Food Engineering*, 215, 84–96.
- 584 Garcia-Montoya, I. A., Cendon, T. S., Arevalo-Gallegos, S., & Rascon-Cruz, Q. (2012). Lactoferrin a
585 multiple bioactive protein: an overview. *Biochimica et Biophysica Acta*, 1820, 226-236.
- 586 Gerberding, S. J., & Byers, C. H. (1998). Preparative ion-exchange chromatography of proteins from dairy
587 whey. *Journal of Chromatography A*, 808, 141–151.
- 588 González-Chávez, S. A., Arévalo-Gallegos, S., & Rascón-Cruz, Q. (2009). Lactoferrin: structure, function
589 and applications. *International Journal of Antimicrobial Agents*, 33, 301.e1–301e8.
- 590 Hirsch, D. B., Baieli, M. F., Urtasun, N., Lazaro-Martinez, J. M., Glisoni, R. J., Miranda, M. V., et al.
591 (2018a). Sulfanilic acid-modified chitosan mini-spheres and their application for lysozyme
592 purification from egg white. *Biotechnology Progress*, 34, 387–396.

- 593 Hirsch, D. B., Urtasun, N., Baieli, M. F., Miranda, M. V., Cascone, O., & Wolman, F. J. (2018b). Dye affinity
594 chromatography: a low-cost tool for protein purification. *Advances in Chemistry Research*. Nova
595 Science Publishers Inc.
- 596 Johansson, B.-L., Belew, M., Eriksson, S., Glad, G., Lind, O., Maloisel, J.-L., et al. (2003). Preparation and
597 characterization of prototypes for multi-modal separation aimed for capture of positively
598 charged biomolecules at high-salt conditions. *Journal of Chromatography A*, *1016*, 35–49.
- 599 Kallberg, K., Johansson, H. O., & Bulow, L. (2012). Multimodal chromatography: an efficient tool in
600 downstream processing of proteins. *Biotechnology Journal*, *7*, 1485–1495.
- 601 Kasai, M. R., Arul, J., & Charlet, G. (2000). Intrinsic viscosity–molecular weight relationship for chitosan.
602 *Journal of Polymer Science Part B: Polymer Physics*, *38*, 2591–2598.
- 603 Kilara, A., & Vaghela, M. N. (2018). Whey proteins. In Y. Yada (Ed.), *Proteins in food processing* (pp. 93-
604 126). Chichester, UK: Woodhead Publishing.
- 605 Kumar Gupta, V., Agarwal, S., Asif, M., Fakhri, A., & Sadeghi, N. (2017). Application of response surface
606 methodology to optimize the adsorption performance of a magnetic graphene oxide
607 nanocomposite adsorbent for removal of methadone from the environment. *Journal of Colloid
608 and Interface Science*, *497*, 193–200.
- 609 Kumar, M. N. V. R. (2000). A review of chitin and chitosan applications. *Reactive & Functional Polymers*,
610 *46*, 1–27.
- 611 Kumari, S., Kumar Annamareddy, S. H., Abanti, S., & Kumar Rath, P. (2017). Physicochemical properties
612 and characterization of chitosan synthesized from fish scales, crab and shrimp shells.
613 *International Journal of Biological Macromolecules*, *104*, 1697–1705.
- 614 Langmuir, I. (1917). The constitution and fundamental properties of solids and liquids. *Journal of the
615 Franklin Institute*, *183*, 102–105.

- 616 Lázaro-Martínez, J. M., Rodríguez-Castellón, E., Vega, D., Monti, G. A., & Chattah, A. K. (2015). Solid-
617 state studies of the crystalline/amorphous character in linear poly(ethylenimine hydrochloride)
618 (PEI·HCl) polymers and their copper complexes. *Macromolecules*, *48*, 1115–1125.
- 619 Legrand, D. (2016). Overview of lactoferrin as a natural immune modulator. *Journal of Pediatrics*, *173*,
620 S10–S15.
- 621 Liang, Y., Wang, X., Wu, M., & Zhu, W. (2011). Simultaneous isolation of lactoferrin and lactoperoxidase
622 from bovine colostrum by SPEC 70 SLS cation exchange resin. *International Journal of*
623 *Environmental Research and Public Health*, *8*, 3764–3776.
- 624 Manzoni, P. (2016). Clinical benefits of lactoferrin for infants and children. *Journal of Pediatrics*, *173*,
625 S43–S52.
- 626 Mariotti, M. P., Yamanaka, H., Araujo, A. R., & Trevisan, H. C. (2008). Hydrolysis of whey lactose by
627 immobilized β -galactosidase. *Brazilian Archives of Biology and Technology*, *51*, 1233–1240.
- 628 Martínez Álvarez, L. M., Lo Balbo, A., Mac Cormack, W. P., & Ruberto, L. A. M. (2015). Bioremediation of
629 a petroleum hydrocarbon-contaminated Antarctic soil: Optimization of a biostimulation strategy
630 using response-surface methodology (RSM). *Cold Regions Science and Technology*, *119*, 61–67.
- 631 Mollea, C., Marmo, L., & Bosco, F. (2013). Valorisation of cheese whey, a by-product from the dairy
632 industry. In I. Muzzalupo (Ed.), *Food industry*. London, UK: IntechOpen.
- 633 Nicolás, P., Ferreira, M., & Lassalle, V. (2018). A review of magnetic separation of whey proteins and
634 potential application to whey proteins recovery, isolation and utilization. *Journal of Food*
635 *Engineering*, *246*, 7–15.
- 636 Nicolás, P., Ferreira, M. L., & Lassalle, V. (2019). Magnetic solid-phase extraction: A nanotechnological
637 strategy for cheese whey protein recovery. *Journal of Food Engineering*, *263*, 380–387.

- 638 Pochet, S., Arnould, C., Debournoux, P., Flament, J., Rolet-Repecaud, O., & Beuvier, E. (2018). A simple
639 micro-batch ion-exchange resin extraction method coupled with reverse-phase HPLC (MBRE-
640 HPLC) to quantify lactoferrin in raw and heat-treated bovine milk. *Food Chemistry*, *259*, 36–45.
- 641 Prado, H. J., & Matulewicz, M. C. (2014). Cationization of polysaccharides: A path to greener derivatives
642 with many industrial applications. *European Polymer Journal*, *52*, 53–75.
- 643 Price, J. (2019). History of the development and application of whey protein products. In H. C. Deeth &
644 N. Bansal (Eds.), *Whey proteins: From milk to medicines* (pp. 51–95). Oxford, UK: Academic
645 Press.
- 646 Ravikumar, K., Krishnan, S., Ramalingam, S., & Balu, K. (2007). Optimization of process variables by the
647 application of response surface methodology for dye removal using a novel adsorbent. *Dyes and*
648 *Pigments*, *72*, 66–74.
- 649 Roh, I. J., & Kwon, I.-C. (2002). Fabrication of a pure porous chitosan bead matrix. *Journal of Biomaterials*
650 *Science, Polymer Edition*, *13*, 769–782.
- 651 Senra, T. D. A., Campana-Filho, S. P., & Desbrières, J. (2018). Surfactant-polysaccharide complexes based
652 on quaternized chitosan. Characterization and application to emulsion stability. *European*
653 *Polymer Journal*, *104*, 128–135.
- 654 Shariatnia, Z., & Jalali, A. M. (2018). Chitosan-based hydrogels: Preparation, properties and applications.
655 *International Journal of Biological Macromolecules*, *115*, 194–220.
- 656 Shojaeimehr, T., Rahimpour, F., Schwarze, M., Repke, J. U., Godini, H. R., & Wozny, G. (2018). Use of
657 RSM for the multivariate, simultaneous multiobjective optimization of the operating conditions
658 of aliphatic carboxylic acids ion-exclusion chromatography column: Quantitative study of
659 hydrodynamic, isotherm, and thermodynamic behavior. *Journal of Chromatography B*, *1083*,
660 146–159.

- 661 Subramanian, A., & Hommerding, J. (2005). The use of confocal laser scanning microscopy to study the
662 transport of biomacromolecules in a macroporous support. *Journal of Chromatography B*, *818*,
663 89–97.
- 664 Urtasun, N., Baieli, M. F., Hirsch, D. B., Martínez-Ceron, M. C., Cascone, O., & Wolman, F. J. (2017).
665 Lactoperoxidase purification from whey by using dye affinity chromatography. *Food and*
666 *Bioproducts Processing*, *103*, 58–65.
- 667 Urtasun, N., Baieli, M. F., Hirsch, D. B., Miranda, M. V., Cascone, O., & Wolman, F. J. (2018). Challenges in
668 dairy whey protein purification. In N. E. Labrou, E. G. Chronopoulou & F. Atava (Eds.), *Handbook*
669 *on protein purification: Industry challenges and technological developments*. Hauppauge, NY,
670 USA: Nova Science Publishers Inc.
- 671 Wakabayashi, H., Oda, H., Yamauchi, K., & Abe, F. (2014). Lactoferrin for prevention of common viral
672 infections. *Journal of Infection and Chemotherapy*, *20*, 666–671.
- 673 Wakabayashi, H., Yamauchi, K., & Takase, M. (2006). Lactoferrin research, technology and applications.
674 *International Dairy Journal*, *16*, 1241–1251.
- 675 Wu, X. L., & Zilm, K. W. (1993). Complete spectral editing in CPMAS NMR. *Journal of Magnetic*
676 *Resonance, Series A*, *102*, 205–213.
- 677 Yang, Y., & Geng, X. (2011). Mixed-mode chromatography and its applications to biopolymers. *Journal of*
678 *Chromatography A*, *1218*, 8813–8825.
- 679 Yang, Y., Wang, Y., Niu, R., Lu, J., Zhu, X., & Wang, Y. (2016). Preparation and characterization of chitosan
680 microparticles for immunoaffinity extraction and determination of enrofloxacin. *International*
681 *Journal of Biological Macromolecules*, *93*, 783–788.
- 682 Yoshida, S. (1989). Preparation of lactoferrin by hydrophobic interaction chromatography from milk acid
683 whey. *Journal of Dairy Science*, *72*, 1446–1450.

- 684 Yoshida, S., & Ye, X. (1991). Isolation of lactoperoxidase and lactoferrins from bovine milk acid whey by
685 carboxymethyl cation exchange chromatography. *Journal of Dairy Science*, 74, 1439–1444.
- 686 Zhang, K., & Liu, X. (2016). Mixed-mode chromatography in pharmaceutical and biopharmaceutical
687 applications. *Journal of Pharmaceutical and Biomedical Analysis*, 128, 73–88.
- 688 Zhao, G., Dong, X. Y., & Sun, Y. (2009). Ligands for mixed-mode protein chromatography: Principles,
689 characteristics and design. *Journal of Biotechnology*, 144, 3–11.
- 690

Figure legends

Fig. 1. Scheme of synthesis reactions for mini-spheres.

Fig. 2. ^{13}C CP-MAS spectra for chitosan-minispheres (A), crosslinked chitosan-minispheres (B) and GTMA-modified chitosan-minispheres (C). The numbers above spectra C correspond to the numbers assigned for the different carbon atoms shown to the right.

Fig. 3. ζ potential at different pH values of disrupted (■) chitosan mini-spheres, (●) chitosan mini-spheres with GTMA and (▲) chitosan mini-spheres with sulfanilic acid

Fig. 4. Maximum adsorption capacity of sulfanilic modified mini-spheres for pure LF at different pH values.

Fig. 5. LF adsorption (%) as function of the matrix amount (mg) and whey pH, keeping the time of adsorption constant at 4 h.

Fig. 6. Elution (%) of (A) LF and (B) total proteins as function of the NaCl concentration (M) and PG concentration (%), keeping the elution buffer pH constant at the determined optimum, pH 7.53 and (C) desirability of the optimisation by maximising LF elution while the total proteins eluted were settled at a target of 1.59%.

Fig. 7. SDS-PAGE (12%) of the LF purification process: lane 1, commercial LF 0.5 mg mL⁻¹; lane 2, molecular mass marker; lane 3, whey 4×; lane 4, pass-through 4×; lane 5, desalted eluate 4×.

Fig. 8. Total whey protein adsorption (%) as function of the matrix amount (mg) and time of adsorption (h).

Fig. 9. Total whey proteins eluted (%) as function of the NaCl concentration (M) and elution buffer pH, keeping the PG concentration constant at the determined optimum of 50%.

Fig. 10. SDS-PAGE (12%) of the WPI recovery: lane 1, molecular mass marker; lane 2, desalted eluate; lane 3, pass-through; lane 4, whey.

Table 1

Factor codification for the optimisation of the LF purification process.

Factor	Low level (-1)	Medium level (0)	High level (+1)
Adsorption			
Hydrated matrix amount (A)	25 mg	62.5 mg	100 mg
Adsorption time (B)	0.5 h	2.25 h	4 h
pH (C)	6.0	7.5	9.0
Elution			
pH (A)	3.0	6.0	9.0
NaCl (B)	0.0 M	1.0 M	2.0 M
Propylene glycol (C)	0.0%	25.0%	50.0%

Table 2

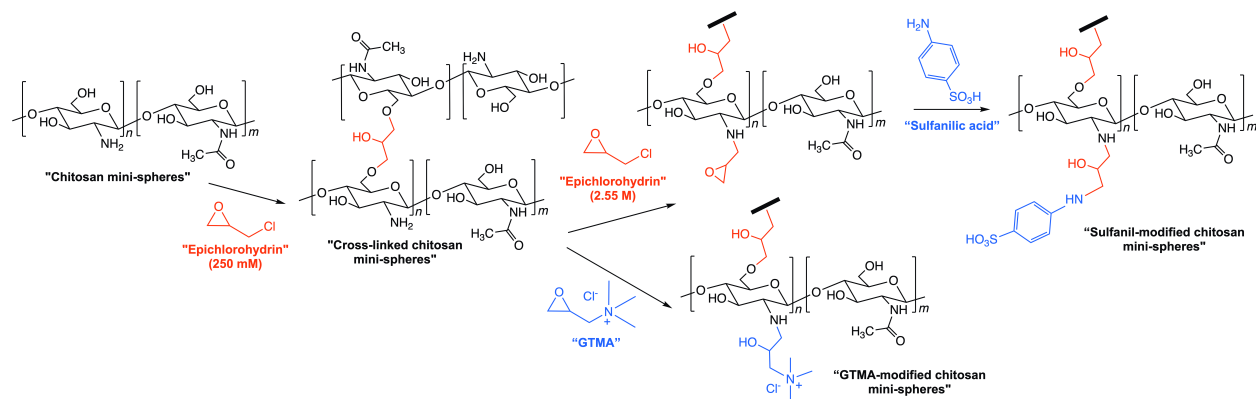
Factor codification for the optimisation of the WPI recovery process.

Factor	Low level (-1)	Medium level (0)	High level (+1)
Adsorption			
Hydrated matrix amount (A)	100 mg	550 mg	1000 mg
Adsorption time (B)	0.5 h	2.25 h	4 h
Elution			
pH (A)	4.0	5.5	7.0
NaCl (B)	0.0 M	1.0 M	2.0 M
Propylene glycol (C)	0.0%	25.0%	50.0%

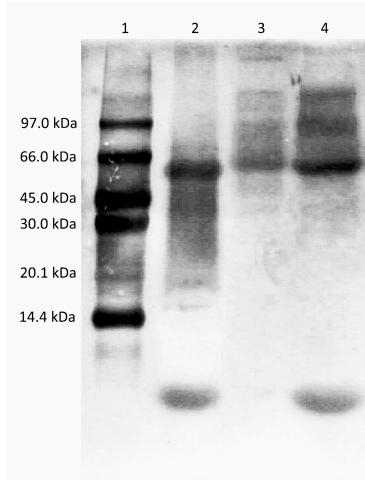
Table 3

Sequence purification process results.

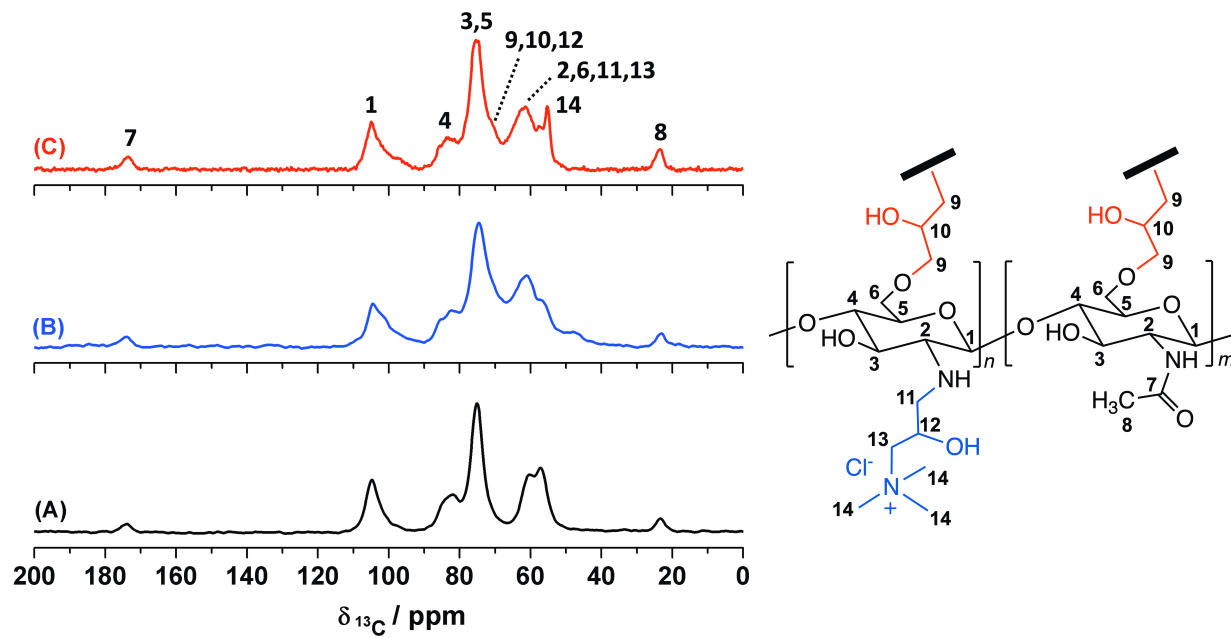
Step	Initial total protein (mg mL ⁻¹)	Initial LF (mg mL ⁻¹)	Adsorption (%)	Elution (%)
LF purification step	7.29 ± 0.52	0.14 ± 0.01	75.35 ± 5.79	82.73 ± 1.05
WPI recovery step	5.97 ± 0.09	-	52.09 ± 1.34	87.30 ± 6.13

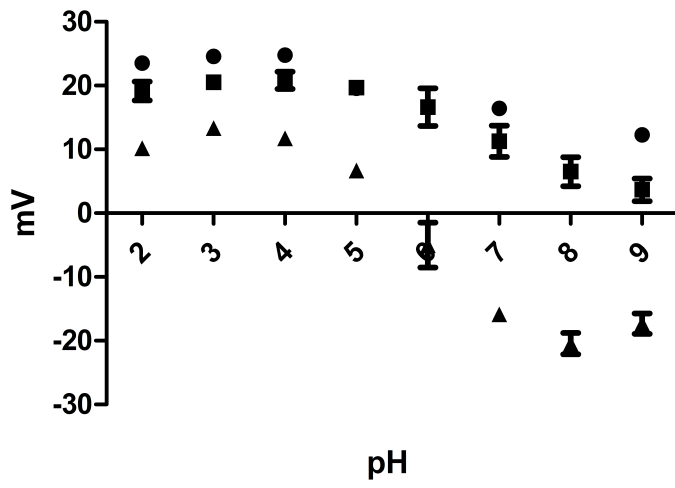


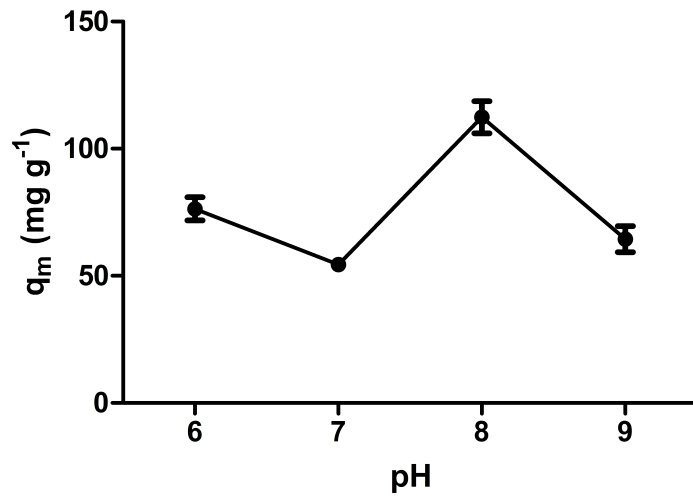
Journal Pre-proof

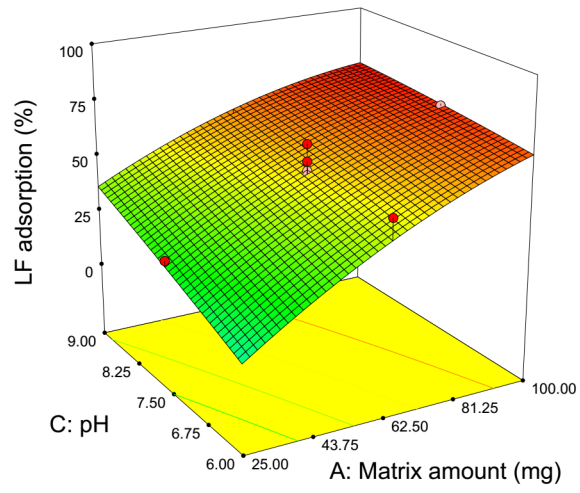


Journal Pre-proof

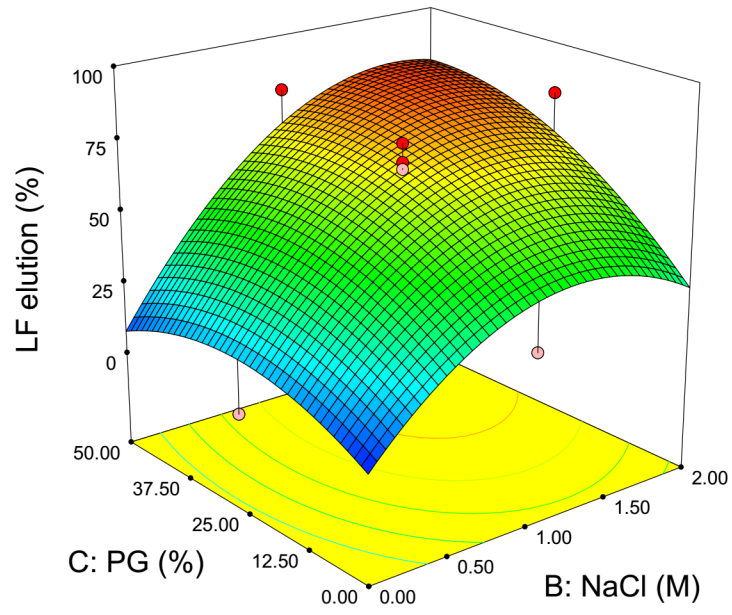


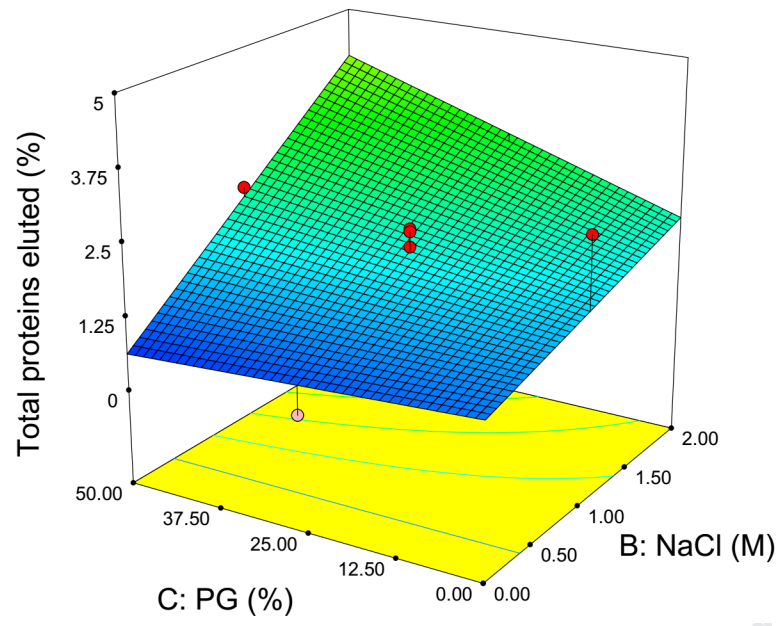


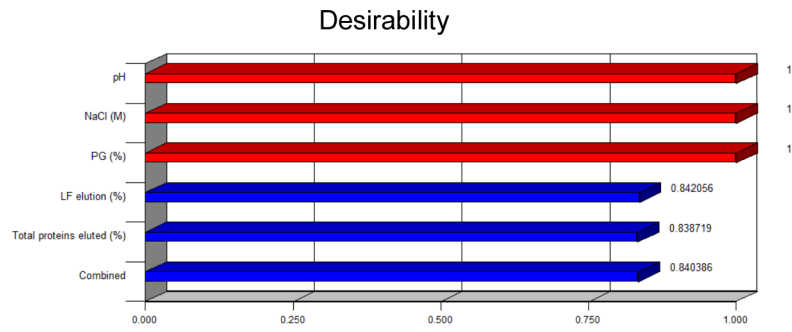




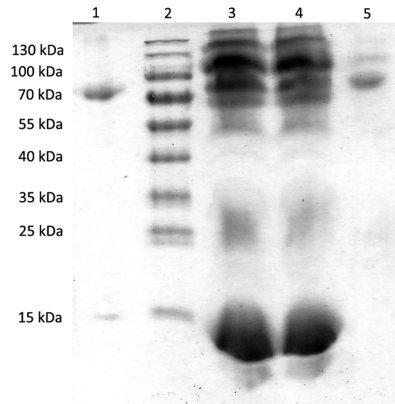
Journal Pre-proof



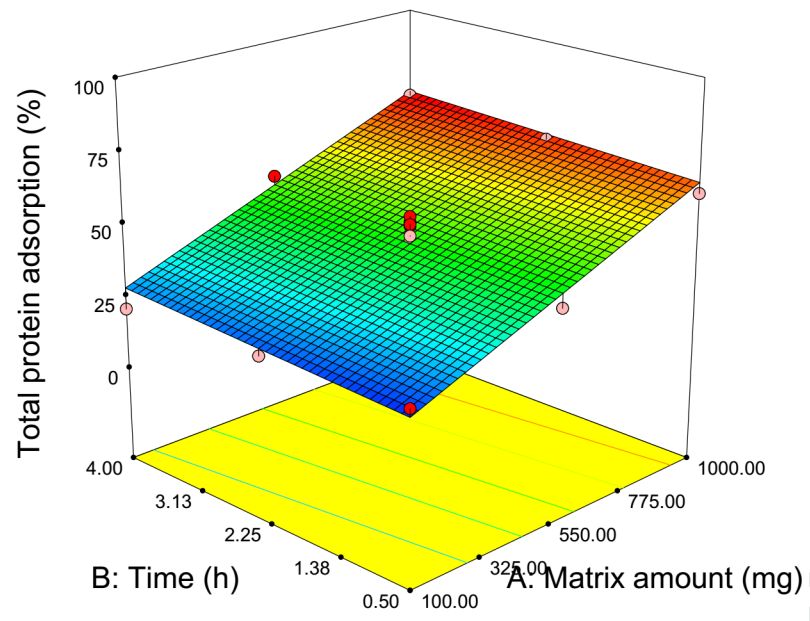


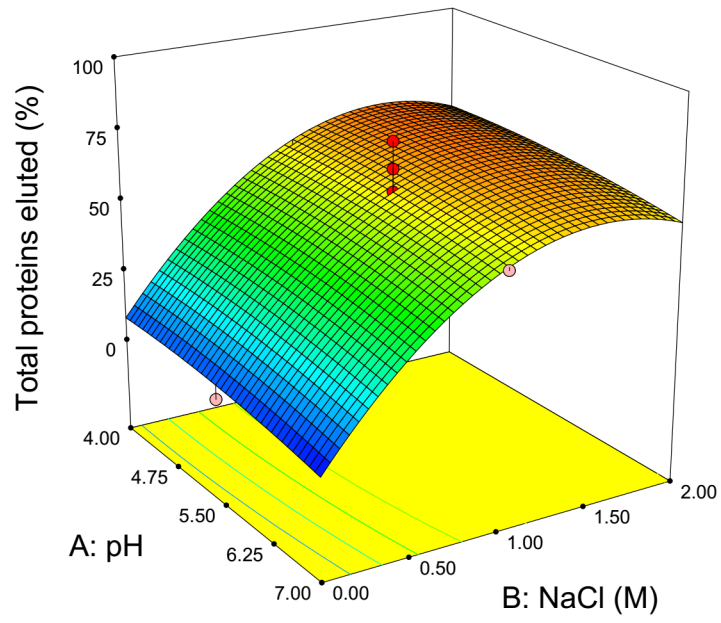


Journal Pre-proof



Journal Pre-proof





Author contributions

DBH, conceptualisation, design, experimentation, writing; FJW, conceptualisation, design, manuscript review; LMMA, statistical analysis; MFB, NU, data analysis and validation. JMLM, RJG, experimentation; MVM, OC, manuscript review.

Journal Pre-proof